Two-Dimensional to Three-Dimensional Transition in Soap Films Demonstrated by Microrheology

V. Prasad and Eric R. Weeks

Department of Physics, Emory University, Atlanta, Georgia 30322, USA

(Received 29 July 2008; published 29 April 2009)

We follow the diffusive motion of colloidal particles of diameter d in soap films of varying thickness h with fluorescence microscopy. Diffusion constants are obtained both from one- and two-particle microrheological measurements of particle motion in these films. These diffusion constants are related to the surface viscosity of the interfaces comprising the soap films, by means of the Trapeznikov approximation and Saffman's equation for diffusion in a 2D fluid. Unphysical values of the surface viscosity are found for thick soap films ($h/d > 7 \pm 3$), indicating a transition from 2D to 3D behavior.

DOI: 10.1103/PhysRevLett.102.178302 PACS numbers: 47.57.Bc, 68.15.+e, 87.16.D−, 87.85.gf

A soap film is a thin layer of fluid stabilized by two surfactant layers that buffer it from air phases above and below. In the early 18th century, Sir Isaac Newton measured the thickness of the fluid layer to ~10 nm precision [1]. Because of the similarity of thin "Newton black films" to planar lipid bilayers, soap films have been proposed as models for cell membranes [2]. The analogy with membranes extends to considering a thin soap film as a 2D fluid [3]. This has motivated the use of soap films to study turbulence in 2D [4,5], as well as informing the physics of drainage in foams [6]. However, soap films have a nonzero thickness, and presumably under some conditions the model of the film as a 2D fluid is inappropriate.

A previous study by Cheung *et al.* [3] quantified the hydrodynamics of a single soap film for the special case where the diameter d of embedded tracer particles was the same as the thickness h of the film. The relative diffusion of pairs of particles depended logarithmically on the separation between the particles, indicating 2D fluidlike behavior. Clearly, for thicker films where $h \gg d$, 3D behavior must be recovered, but this has not been demonstrated in any study to date.

In this Letter, we use the thermal motion of embedded particles to study soap films of varying thickness h, to clarify the relative importance of 2D and 3D hydrodynamics. For small particles in thick films ($h/d > 7$), the measured particle diffusivity is similar to free 3D diffusion in the fluid comprising the film. For thin films ($h/d < 7$), particles diffuse noticeably faster, suggesting that particle drag is more due to 2D hydrodynamics with an effective 2D viscosity. Measurements of the correlated motion of pairs of particles show that *all* soap films have 2D-like long-range correlations. The classic Trapeznikov approximation [7] connects the 2D and 3D properties of the film by modeling the soap film as a 2D interface with an effective surface viscosity $\eta_{s,\mathrm{eff}}$ given by

$$\eta_{s,\mathrm{eff}} = \eta_{\mathrm{bulk}} h + 2\eta_{\mathrm{int}} \quad (1)$$

in terms of the 3D viscosity η_{bulk} of the fluid in the film, and the 2D surface viscosity η_{int} of the surfactant layers; see Fig. 1. Our results show that Eq. (1) and Fig. 1 are valid for thin films but not for thick films where 3D hydrodynamics becomes important. These observations lead us to conclude that a transition from 2D fluid to 3D bulk behavior occurs at around $h/d \approx 7 \pm 3$, the first experimental demonstration of such a transition.

We use mixtures of water, glycerol, and the commercially available dishwashing detergent Dawn to prepare our soap films. This particular brand was chosen as it allows us to compare our results with previous work [3,6,8]. The concentration of Dawn is kept fixed at 2% by weight in our soap solutions to maintain a constant interfacial viscosity η_{int} for all films. The fluid viscosity η_{bulk} in our films is controlled by changing the ratio of water and glycerol in the soap solutions. Fluorescent polystyrene spheres (molecular probes, carboxyl modified, $d = 210$ or 500 nm) are added as tracer particles.

Stable soap films are created by dipping and drawing out a circular stainless steel frame of thickness 1 mm from the soap solutions. The frame is enclosed in a chamber that minimizes convective effects in the soap film while maintaining its relative humidity. We then image the particles by fluorescence microscopy; soap films containing 500 nm particles are imaged with a 20× objective (numerical aperture = 0.4, 465 nm/pixel) while those with 210 nm particles are imaged with a 40× objective (numerical aperture = 0.55, 233 nm/pixel). For each sample, movies of duration ~30 s are recorded with a CCD camera that has a 640 × 486 pixel resolution, at a frame rate of 30 Hz. After each movie, we transfer the film to a spectrophotom-

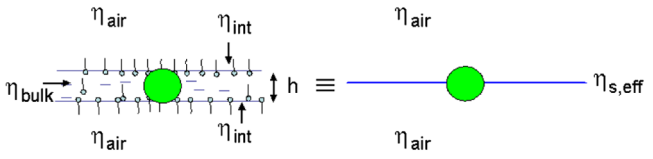

FIG. 1 (color online). Schematic of the Trapeznikov approximation, where the entire soap film is approximated as a single interface in contact with bulk air phases.

eter and its thickness h is determined from the transmitted intensity [9]. The movies are then analyzed by particle tracking to obtain the positions of the tracers. From the particle positions, we determine their displacements by the relation $\Delta\vec{r}(t,\tau) = \vec{r}(t+\tau) - \vec{r}(t)$, where t is the absolute time and τ is the lag time. Finally, any global motion is subtracted from these displacements to eliminate the remnant effects of convective drift caused by the air phases that contact the soap film.

To quantify particle motion, we calculate the mean square displacements (MSDs) $\langle \Delta r^2 \rangle$ as a function of the lag time τ. Figure 2 shows measurements of $\langle \Delta r^2 \rangle$ for five different soap films, where h/d ranges from 0.6 to 15. The viscosity η_{bulk} of the fluid layer of these soap films is given in Table I. At long lag times, all the MSDs are linear with respect to τ. This is expected, as both the fluid layer and the interfaces comprising the soap film are viscous. We extract a one-particle self-diffusion coefficient, $D_{s,1p}$, from the measurements according to the equation $\langle \Delta r^2 \rangle = 4D_{s,1p}\tau$. From Table I and Fig. 2 it is clear that increasing both η_{bulk} and h/d tends to slow the diffusion of the particles. Films made from more viscous bulk fluids tend to be thicker (see Table I), and so these single-particle measurements do not clearly distinguish the influence of η_{bulk} and h/d, although it is obvious that increasing η_{bulk} should slow diffusion, and plausible that increasing h/d might also slow diffusion. This latter effect is suggested by comparing films i and j in Fig. 2, which have the same η_{bulk}; the motion is slower for the thicker film j (upward solid triangles). A further suggestion that thicker films result in slower diffusion comes from comparing the motion within the films (solid symbols in Fig. 2) with motion in the 3D fluid solutions the films are made from (open symbols in Fig. 2). For a thin film ($h/d = 0.6$, stars) the particle motion is much faster in the soap films than in the corresponding 3D solution. For the thickest films we study ($h/d \approx 10$–15, solid diamonds and triangles) the motion in the soap film is comparable to the motion in the corresponding 3D solution (open diamonds).

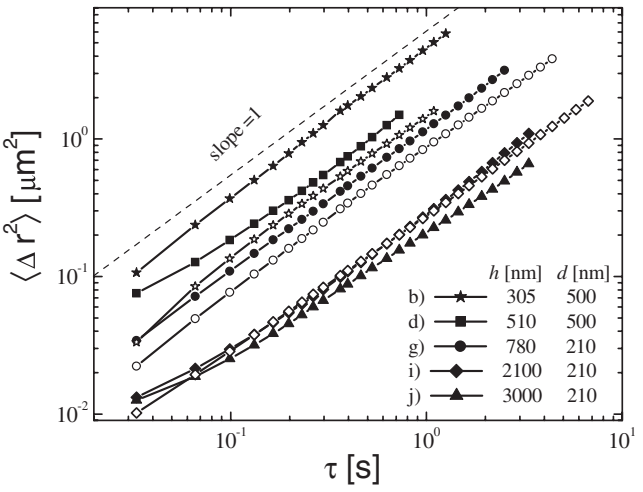

FIG. 2. The solid symbols are the mean square displacements for five soap films with increasing h/d ratios. See Table I for the viscosities η_{bulk} that correspond to these films. The open symbols represent data from the bulk (3D) solutions used to make the soap films for four cases (b, g, i/j).

To further understand the hydrodynamics and how particle motion compares in thick and thin films, we use the correlated motions of particles [10,11] to probe flow fields in these soap films. We look at the product of particle displacements $D_{rr}(R,\tau) = \langle \Delta r_r^i(t,\tau)\Delta r_r^j(t,\tau)\delta[R - R^{ij}(t)]\rangle_{i\neq j,t}$, where i, j are particle indices, the subscripts r represent motion parallel to the line joining the centers of particles, and R^{ij} is the separation between particles i and j. Similar to [11], we observe $D_{rr} \sim \tau$, which enables the estimation of a τ-independent quantity $\langle D_{rr}/\tau \rangle_\tau$, depending only on R and having units of a diffusion constant.

In Fig. 3 we show $\langle D_{rr}/\tau \rangle$ as a function of the separation R for the five soap films described in Fig. 2, with an additional data set from Ref. [3] included. The motion of a tracer particle creates a flow field in the soap film that affects the motion of other particles, and the correlation function indicates the spatial extent of this flow field. The dashed line in Fig. 3 represents the form of the correlation function in a 3D fluid [10]; it is clear that the motion is correlated over larger distances in soap films than in 3D. This long-ranged behavior is characteristic of 2D fluids [12,13]. Further, similar to the trend seen in the MSDs, increasing h/d and η_{bulk} lowers the value of the correlation function $\langle D_{rr}/\tau \rangle$ for the same separation R. As $\langle D_{rr}/\tau \rangle$ dimensionally represents a diffusion constant, slower diffusion decreases its magnitude. Finally, the correlation functions for all six soap films are similar in shape. This is evident from the form of the function, $A \ln R + B$ that has been used to empirically fit all the six curves.

The data set from Cheung *et al.* [3] (open hexagons) requires explanation. In their Letter, the data were presented as a two-particle MSD, $\langle \Delta R^2 \rangle = \langle \{[r_j(t+\tau) - r_i(t+\tau)] - [r_j(t) - r_i(t)]\}^2 \rangle$, which measures the relative

TABLE I. Parameters for all the soap films described in this Letter. η_{bulk} (determined from diffusivity measurements in bulk solutions) has an error of ±5%, and values of h and d are certain to within ±2%. The uncertainties in η_{int}, derived from Eqs. (1) and (2), are given in parentheses.

η_{bulk} (mPa · s)	h (nm)	d (nm)	$\eta_{\text{int}}(1p)$ (nPa · m · s)	$\eta_{\text{int}}(2p)$ (nPa · m · s)
a. 2.0 [3]	400	400	0.20 (±0.03)	0.47 (±0.06)
b. 2.3	305	500	0.63 (±0.06)	1.02 (±0.10)
c. 3.0	640	500	0.49 (±0.09)	0.62 (±0.12)
d. 6.0	510	500	0.89 (±0.2)	0.84 (±0.2)
e. 10.0	1340	500	0.34 (±0.5)	2.26 (±0.7)
f. 25.0	1100	500	−0.30 (±0.9)	4.35 (±1.5)
g. 10.0	780	210	0.12 (±0.26)	1.64 (±0.4)
h. 25.0	2184	210	−8.92 (±1.3)	27.2 (±4)
i. 30.0	2100	210	−10.6 (±1.5)	25.0 (±4)
j. 30.0	3000	210	−15.5 (±2.1)	65.2 (±8)

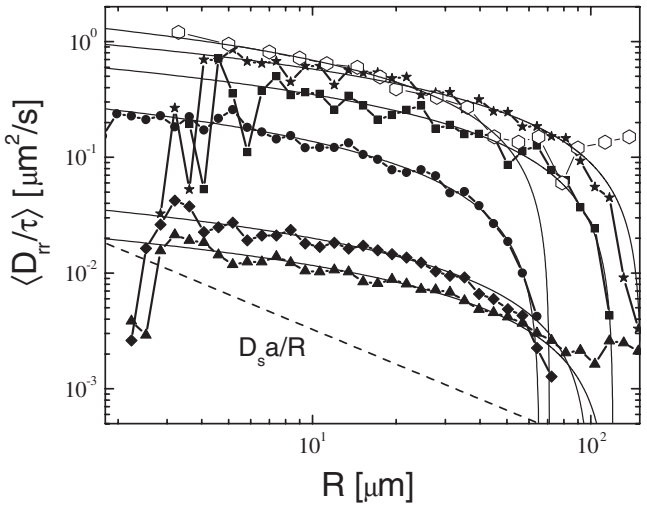

FIG. 3. Two-particle longitudinal correlation function $\langle D_{rr}/\tau\rangle$ for the five soap films described in Fig. 2, symbols being the same. An additional data set from [3] has been included (open hexagons). Solid lines are empirical fits to the data of the form $A \ln R + B$. The dashed line is the form of the correlation function expected for a 3D fluid with $\eta_{\text{bulk}} = 6.5$ mPa · s (squares).

diffusion between particles i and j. This was done for a fixed $\tau(= 1/30$ s), and the resulting relative diffusion decomposed into two components $\langle \Delta R^2\rangle = \langle \Delta R_{\parallel}^2\rangle + \langle \Delta R_{\perp}^2\rangle$, representing displacements parallel and perpendicular to the lines joining the centers of the particles. It is then straightforward to show that $\langle D_{rr}/\tau\rangle = (2\langle \Delta r_r^2\rangle - \langle \Delta R_{\parallel}^2\rangle)/2\tau \approx (\langle \Delta r^2\rangle - \langle \Delta R_{\parallel}^2\rangle)/2\tau$ [14]. We plot the data in this form in Fig. 3, using $\tau = 1/30$ s.

The data shown in Fig. 3 can be used to extract a single-particle self-diffusion constant $D_{s,2p}$, but now measured from two-particle correlations. This is done by extrapolating the correlation functions $\langle D_{rr}/\tau\rangle$ to $R = d/2$; the single-particle diffusion constant must be recovered from the two-particle measurement when extrapolated to the particle radius [10]. We then deduce that $D_{rr}(R = d/2, \tau) = \langle \Delta r_r^2\rangle \approx 2D_{s,2p}\tau$ [14] and use the fitting functions shown in Fig. 3 to determine the value of $D_{s,2p}$ for each soap film. However, this extrapolation process has limitations: nearby particles at interfaces can have strong interactions, either electrostatic or through capillary forces. Our particle concentration was chosen to have spheres be no closer than $R \sim 5d$, to avoid such effects.

We compare the diffusion constants obtained from our two methods in Fig. 4(a). The two diffusion constants agree with each other for thin soap films while for thicker films, the deviation from equality lies beyond experimental error (points h, i, and j). These results can be interpreted using the Trapeznikov approximation described in Fig. 1, so that our system reduces to that of a particle diffusing at an interface in contact with bulk air phases. The diffusion of a disk or sphere [15] at such an interface has been described

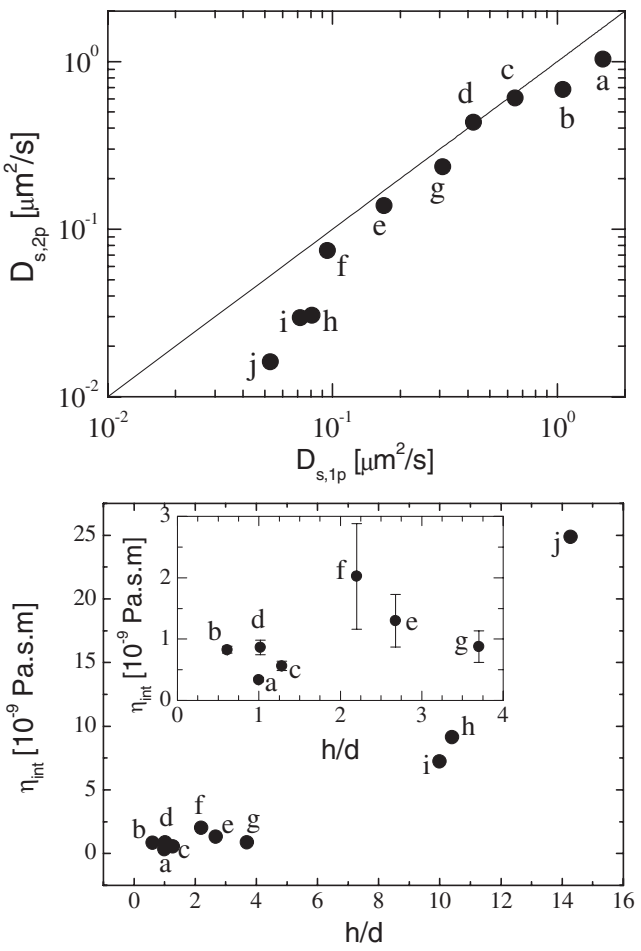

FIG. 4. (a) Two-particle diffusion constant $D_{s,2p}$ plotted against the one-particle $D_{s,1p}$ for the six soap films described in Figs. 2 and 3. Four additional data sets have been included, details of which are given in Table I. The straight line indicates equality between the diffusion constants. Errors in $D_{s,1p}$ and $D_{s,2p}$ are $\pm 5\%$, similar to that in η_{bulk}, and are smaller than the size of the symbols in the figure. (b) Interfacial viscosity η_{int} as a function of h/d. Inset: Magnified view of η_{int} for $h/d < 4$, with error bars included.

by Saffman [16] and is given by

$$D_s = \frac{k_B T}{4\pi\eta_{s,\text{eff}}}\left[\ln\left(\frac{2\eta_{s,\text{eff}}}{\eta_{\text{air}} d}\right) - \gamma_E\right], \tag{2}$$

where η_{air} is the viscosity of the bulk air phases and γ_E is Euler's constant. Equation (2) holds if $2\eta_{s,\text{eff}} \gg \eta_{\text{air}} d$, which is true for our data due to the low value of the air viscosity ($\eta_{\text{air}} = 0.017$ mPa · s).

We now attempt to determine the interfacial viscosity of the surfactant layers by using Eq. (2) to convert measurements of $D_{s,1p}$ and $D_{s,2p}$ into $\eta_{s,\text{eff}}$, and then using Eq. (1) to determine $\eta_{\text{int}} = 1/2(\eta_{s,\text{eff}} - \eta_{\text{bulk}} h)$. For all films, we average $D_{s,1p}$ and $D_{s,2p}$ to determine η_{int}, which is plotted in Fig. 4(b) as a function of h/d. For the thin films the interfacial viscosity shows roughly constant behavior while for thick films the variation in η_{int} is quite pro-

nounced beyond the experimental uncertainty in the measurements (see Table I). The inset to Fig. 4(b) shows a magnified view of the interfacial viscosity for $h/d < 4$, where it is clear that η_{int} is nearly constant with an average value of 0.97 ± 0.55 nPa $\cdot$ s $\cdot$ m. This is expected because the same concentration of Dawn surfactant has been used in all these soap films.

For thick films, the one-particle measurements $D_{s,1p}$ give large *negative* values of η_{int} (refer to Table I) implying that the single-particle diffusivities are significantly faster than that predicted by Eqs. (1) and (2). From Fig. 2, it is clear that the 3D Stokes-Einstein equation for diffusion, $D_{s,1p} = k_B T/(3\pi\eta_{\text{bulk}} d)$, is sufficient to explain the motion of the probe particles in thicker soap films, without the need to invoke Saffman's equation. This makes sense, as in the limit of a 3D system ($h \to \infty$), Eq. (1) predicts an infinite surface viscosity, which has no physical meaning. The apparent negative values of η_{int} for $h/d > 7$ indicate that the 3D limit is already evident for films of this thickness. In contrast with the one-particle measurements, the two-particle measurements in thick films give large *positive* values of η_{int} (see Table I), again contradictory to the low values determined in thin films. An alternate way to state this is that the Trapeznikov approximation predicts an effective surface viscosity that is too small, if we use η_{int} based on the thin film measurements.

This leaves us with a puzzle; even for these thick films the two-particle correlation functions are long ranged, indicating that the soap films behave like a 2D fluid. In fact, the behavior of the correlation functions as a function of R for all soap films can be explained by considering the following. Locally, the films likely behave as a 3D fluid [17]. We hypothesize that the correlation functions in the thick films would then decay as $1/R$ at very short separations ($d/2 < R < h$) but more slowly at larger separations ($R > h$) . The extrapolation of D_{rr} to $R = d/2$ thus underpredicts $D_{s,2p}$, explaining the overestimation of η_{int} for the thick films. At intermediate separations, because of conservation of fluid momentum, *all* soap films behave as 2D fluids [17]. Therefore, the correlation functions decay in a logarithmic fashion for those separations, as seen by the form of the fitting functions in Fig. 3. However, the logarithmic divergence of the correlation function is cut off at a length scale where stresses in the air phase from motion of the tracers become important. This length scale, related to $\eta_{s,\text{eff}}/\eta_{\text{air}}$, is the separation at which the correlation functions begin to decay more rapidly, indicating a final crossover to 3D fluidlike behavior.

A question as yet not addressed in this Letter is the positions of the probe particles, especially in cases where $h > d$. The particles could either reside within the films or be bound to one of the interfaces of the film, resulting in a splitting of their mobilities. To eliminate this possibility, we compute the displacements of each individual particle in all our soap films for a fixed τ (data not shown). The histogram of these displacements shows Gaussian statistics as expected for an ensemble of particles undergoing Brownian motion, with every particle having the same local environment and mobility.

Our work describes a transition from 2D to 3D behavior when the thickness of soap films are changed with respect to particle size, at a ratio of $h/d \approx 7 \pm 3$. This particular value of h/d is an empirical determination of when 3D shear gradients in the fluid layer dominate dissipation of stress from the motion of the probe, in comparison to the air phase. For thin films showing 2D behavior, the air phase is crucial for stress dissipation, as demonstrated by the presence of η_{air} in the Saffman equation [Eq. (2)]. In all our films, the interface is relatively *mobile*, that is, η_{int} is small when compared to the contribution from the fluid layer $\eta_{\text{bulk}} h$; changing this will likely change where the transition occurs.

Funding for this work was provided by the National Science Foundation (DMR-0603055) and the Petroleum Research Fund, administered by the American Chemical Society (47970-AC9). We also thank J. Gallivan and S. Topp for assistance with the spectrophotometer.

[1] I. Newton, *Optics* (Dover, New York, 1952), p. 215.
[2] H. T. Tien and A. L. Ottova, J. Membr. Sci. **189**, 83 (2001).
[3] C. Cheung, Y. H. Hwang, X. L. Wu, and H. J. Choi, Phys. Rev. Lett. **76**, 2531 (1996).
[4] W. I. Goldburg, M. A. Rutgers, and X. L. Wu, Physica (Amsterdam) **239A**, 340 (1997).
[5] J. M. Burgess, C. Bizon, W. D. McCormick, J. B. Swift, and H. L. Swinney, Phys. Rev. E **60**, 715 (1999).
[6] H. A. Stone, S. A. Koehler, S. Hilgenfeldt, and M. Durand, J. Phys. Condens. Matter **15**, S283 (2003).
[7] A. A. Trapeznikov, in *Proceedings of the 2nd International Congress on Surface Activity* (Butterworths, London, 1957).
[8] M. A. Rutgers, X. L. Wu, and W. B. Daniel, Rev. Sci. Instrum. **72**, 3025 (2001).
[9] P. D. T. Huibers and D. O. Shah, Langmuir **13**, 5995 (1997).
[10] J. C. Crocker *et al.*, Phys. Rev. Lett. **85**, 888 (2000).
[11] V. Prasad, S. A. Koehler, and E. R. Weeks, Phys. Rev. Lett. **97**, 176001 (2006).
[12] A. J. Levine and F. C. MacKintosh, Phys. Rev. E **66**, 061606 (2002).
[13] H. A. Stone and A. Ajdari, J. Fluid Mech. **369**, 151 (1998).
[14] In this work, we focus on D_{rr}, the correlated motion of two particles along the direction of the line separating them. An additional component $D_{\theta\theta}$ can be computed, where θ indicates the direction of motion perpendicular to this line. Thus the true displacement of a single particle of diameter d should be $D_{rr}(R = d/2, \tau) + D_{\theta\theta}(R = d/2, \tau) = \langle \Delta r_r^2 \rangle + \langle \Delta r_\theta^2 \rangle = \langle \Delta r^2 \rangle = 4D_{s,2p}\tau$. In 2D, $\langle \Delta r_r^2 \rangle \approx \langle \Delta r_\theta^2 \rangle$ and thus $D_{rr}(R = d/2, \tau) \approx 2D_{s,2p}\tau$.
[15] M. Sickert, F. Rondelez, and H. A. Stone, Europhys. Lett. **79**, 66005 (2007).
[16] P. G. Saffman and M. Delbrück, Proc. Natl. Acad. Sci. U.S.A. **72**, 3111 (1975).
[17] H. Diamant (private communication).